PCCP

Imaging H abstraction dynamics in crossed molecular beams: Cl + ROH reactions

Musahid Ahmed, Darcy S. Peterka and Arthur G. Suits*

Chemical Sciences Division, Ernest Orlando Lawrence Berkeley National Laboratory, Berkeley, CA, 94720, USA E-mail: agsuits@lbl.gov

Received 30th September 1999, Accepted 4th November 1999

The crossed beam reactions of ground state $Cl(^2P_{3/2})$ atoms with alcohols (CH_3OH, C_2H_5OH and 2-C_3H_7OH) have been studied using the technique of velocity map imaging (VELMI). The corresponding hydroxyalkyl radical was detected *via* single photon ionization using 157 nm laser light. The double differential cross sections were obtained at collision energies of 8.7 kcal mol^{-1} for methanol, 6.0 and 9.7 kcal mol^{-1} for ethanol and 11.9 kcal mol^{-1} for 2-propanol. In all cases, the scattering was predominantly in the backward–sideways direction suggesting direct rebound dynamics, with varying amounts of sideways scattering. In the case of methanol, the angular distributions were predominantly in the sideways–backward direction with respect to the incoming alcohol beam. Scattering was into the backward hemisphere at the lower collision energy for ethanol, with enhancement of sideways scattering with an increase in collision energy. Isopropanol gave scattering predominantly in the backward direction. Coupling between the translational energy and angular distributions was particularly significant for ethanol at the lower collision energy. All of the translational energy distributions peaked at about 6 kcal mol^{-1} and on average 30–40% of the available energy was deposited into product translation for all the alcohols studied. These results are contrasted with previous H abstraction studies performed on Cl–hydrocarbon systems.

Introduction

Abstraction reactions of hydrogen atoms from hydrocarbons are of great importance in combustion and atmospheric chemistry. This is reflected in numerous publications where the kinetics of these processes have been probed in detail. While rate information provides some insight into the mechanisms of these reactions, it is the dynamics that provides a deeper understanding. For example, free radical abstraction of hydrogen atoms from saturated hydrocarbons and the differing propensities for reaction of primary, secondary, or tertiary H atoms, as well as differing dynamics underlying these pathways, are important for a detailed understanding of combustion chemistry. With the advent of laser technology and development of new techniques in studying such processes, there has been an explosion of studies, particularly for the reactions of O and Cl with saturated hydrocarbons.

The earliest study of the dynamics of H abstraction from saturated hydrocarbons can be traced back to two seminal papers by Andresen and Luntz,[1,2] wherein they probed the dynamics of $O(^3P)$ with a variety of saturated hydrocarbons (neopentane, cyclohexane, and isobutane) using laser induced fluorescence (LIF) in conjunction with crossed molecular beams. They found that the resultant OH rotational state distributions were nearly identical for all the hydrocarbons and decrease rapidly from a peak at the lowest rotational level, suggesting strong dynamical constraints favoring collinearity in the critical region along the reaction pathway. The trends that they observed for the OH rotational distribution have been confirmed in all subsequent studies of H abstraction dynamics—that the newly formed hydride products, regardless of the identity of the hydrocarbon or the attacking atom, are formed rotationally cold. Furthermore they found that the vibrational state distribution of OH depends markedly on the type of hydrogen abstracted, with vibrational excitation increasing dramatically across the series primary to secondary to tertiary, correlating with the increasing exothermicity of the reaction. They interpreted this dynamic behavior as a shift from a repulsive toward a more attractive surface across the series of hydrocarbons studied.

Subsequently the reactions of $O(^3P)$ with a number of organic compounds were studied using similar techniques by a number of groups—notably Kleinermanns and Luntz[3–5] and Whitehead and co-workers.[6,7] Very recently McKendrick and co-workers[8,9] have reinvestigated the reactions of oxygen with a series of hydrocarbons. They confirmed the previous results of Andresen and Luntz, and went on to investigate the reaction of $O(^3P)$ with CH_4 and C_2H_6. They found similar low levels of rotational energy release, suggesting that the previously proposed strong collinear constraint also applied to the smaller hydrocarbons.

The abstraction reaction

$$Cl + RH \rightarrow R^{\cdot} + HCl$$

leads to the formation of a chain propagating hydrocarbon radical whose properties and chemistry are of importance in combustion, atmospheric, and interstellar processes. Zare and co-workers[10–12] have investigated the dynamics of Cl atom reactions with a variety of hydrocarbons using the "photoloc" technique, providing state-resolved differential cross sections for these reactions. The HCl rotational distribution from the reaction of Cl with vibrationally excited methane was characteristically cold, but the scattering was predominantly forward for the vibrationally excited product, and backward for the vibrationless HCl product. Since these experiments were performed on the state-to-state level, the authors showed that even though all the rotational distributions were relatively cold, for the $v = 1$ HCl product, the higher J values were associated with greater back-scattering. Furthermore, with the photoloc technique stereodynamic information can be extracted from the experimental results. Simpson *et al.* report-

DOI: 10.1039/a907877k

ed a significant steric effect for the vibrationally excited methane reaction: reactions yielding HCl($v = 1$) were favored by perpendicular approach of the Cl atoms to the excited C–H stretch. They argued that the association of low rotational excitation with a collinear transition state, as adduced by Andresen and Luntz in the O(^{3}P) reactions and by Flynn and co-workers[13] for the Cl–C_6D_6 reaction, is strictly appropriate only when there is impulsive energy release in the reaction. For the Cl–methane($v = 1$) case, the cold rotational distributions for the forward-scattered $v = 1$ product were attributed instead to a stripping-like mechanism involving large impact parameter collisions.

For the Cl–CD_4 and Cl–C_2D_6 systems,[14] both showed scattering behavior described by the previously mentioned line-of-centers model and both yielded rotationally cold DCl product with little energy in the alkyl fragment. However the product polarizations differed greatly for the two reactions. For the Cl + CD_4 reaction, J_{DCl} was maximally aligned perpendicular to the axis close to the product scattering direction, while for the Cl + C_2D_6 case the J_{DCl} was half-maximally aligned perpendicular to the line-of-centers direction. The authors interpreted these results in terms of the location of the D atom transfer along the reaction coordinate, positing that the D atom transfer for the methane reaction occurs late in the reactive process, while for ethane the reaction occurs earlier near the distance of closest approach. The authors argue that this dynamical behavior is the cause of the large differences in the Arrhenius pre-exponential factors for the two reactions. Previously Zare's group used 2 + 1 REMPI (resonance enhanced multiphoton ionization) to study the HCl distributions and differential cross sections arising from the reaction of Cl with different hydrocarbons. Very recently, Kandel *et al.*[15] probed the differential cross section for the Cl + $C_2H_6 \rightarrow$ Cl + C_2H_5 reaction, using a 2 + 1 REMPI scheme to detect the heavier hydrocarbon radical product. These results were identical to the ones measured using the HCl detection scheme.[16]

While Zare and co-workers have concentrated their efforts on the reaction of Cl with small hydrocarbons, Varley and Dagdigian[17–19] carried out a detailed investigation of the reactions with propane, isobutane, selectively deuterated propane, and also methane. State-resolved differential cross sections were obtained using a technique similar to the photoloc approach—HCl was predominantly back-scattered in the isobutane reaction, and the vibrational population ratios were very similar for propane and isobutane. Andresen and Luntz observed very different behavior for the O(^{3}P) reaction. Varley and Dagdigian's result for partially deuterated propane showed that abstraction of the D atoms (as the primary substituents) led to sideways scattered DCl product, while abstraction of the H atom (secondary substituents) led to a more isotropic angular distribution, yet still favoring the backward direction.

Elegant as these state-resolved experiments are, one must exercise caution in interpreting the results involving polyatomic systems. Often the distributions obtained are blind to the internal energy in the undetected product, so frequently the assumption is made that the undetected product is internally cold, an assumption that may not be valid. Suits and co-workers have employed a novel alternative technique to probe the hydrocarbon radicals formed in the abstraction reactions of Cl with hydrocarbons. They used the crossed molecular beam technique in conjunction with tunable VUV synchrotron radiation for product photoionization to study the dynamics of Cl reactions with propane[20] and pentane.[21] The use of tunable undulator radiation offered them a unique combination of universality and selectivity in product detection which was not possible with traditional electron impact ionization normally used in such crossed beam studies. The results for propane showed two distinct reaction mechanisms that depended on the impact parameter of the reactive collision. Large impact parameter collisions proceed *via* a stripping mechanism resulting in forward-scattered products with very little momentum change in going from reactant to product. The authors argue that the stripping reactions are most likely dominated by abstraction of secondary hydrogen atoms. The second mechanism, involving smaller impact parameter collisions, leads to direct reaction consistent with a preference for a collinear transition state geometry, C–H–Cl.

In the case of pentane, Hemmi and Suits[21] found that the energy and angular distributions were strongly coupled, with the forward-scattered pentyl radical formed extremely cold, while the back-scattered radicals were formed leaving nearly 15 kcal mol^{-1} in internal energy of the products. The result for the forward-scattered products was largely consistent with previous studies of Cl–hydrocarbon reaction dynamics (spectator stripping mechanism). In contrast the results for the back-scattered products showed a much smaller fraction of the available energy in translation, compared with earlier studies. They invoked the direct involvement of the carbon skeleton in the collision process. Pentane contains a higher density of states compared to propane; furthermore there is an excellent match between the collision time and the bending vibrational period, allowing efficient coupling between the collision energy and the internal modes of the molecule.

While there have been a number of detailed dynamical studies performed on H abstractions from saturated hydrocarbons, it is surprising that analogous studies of H abstraction from alcohols are so rare. Alcohol oxidation has broad practical significance. Alcohols, saturated and unsaturated, are emitted into the atmosphere by vegetation.[22] These biogenic emissions play an important role in the chemistry of the troposphere, especially in rainforest eco-systems such as the Amazon. Saturated alcohols have long been used in large quantities as industrial solvents. Most importantly, from the earliest days of the internal combustion engine—N. A. Otto used ethanol in his classic combustion engine tests in 1897—alcohols have been used as fuels and fuel additives. Recently there has been greatly renewed interest in alcohol-based combustion systems[23] as an alternative to gasoline since the former are thought to be environmentally more benign.[24]

There have been a few cases in the literature where the dynamics of reaction of electronically excited atoms with alcohols have been documented. Goldstein and Wiesenfeld[25] studied the reaction of O(^{1}D) with methanol and ethanol and its deuterated analogs, and characterized the OH and OD product ratios and vibrational distributions using LIF. Their results show that the primary site of O(^{1}D) attack upon the alcohols is the O–H bond, although some attack upon the C–H bond was also observed. They suggested an insertion/elimination mechanism and concluded that abstraction processes were minor based on the low vibrational excitation of OH(OD). Very recently Umemoto *et al.*[26] examined the reaction pathways of N(^{2}D) with methanol and its isotopomers using LIF pump-and-probe techniques. They observed ground state NH and OH radicals with the nascent state distributions of these radicals being non-statistical, suggesting that the intermediate decomposes before energy randomization. These examples have been included here to contrast the differences in the dynamics of electronically excited atoms and ground state reactants. The only dynamic study to date of ground state reactions with alcohols was performed by Neumark and co-workers.[27] They studied fluorine atom reactions with methanol and ethanol using negative ion transition state spectroscopy. It should be pointed out that the dynamics of F atom reactions with alcohols are not representative across the halogen series, since the large exothermicities associated with these open channels are not available to other halogens or hydroxyl radicals.

We have undertaken a series of experiments to study the dynamics of H abstraction from alcohols using crossed molec-

ular beams in conjunction with velocity map imaging (VELMI); a preliminary report of our study of the methanol reaction has recently been submitted.[28] Ion imaging is a multiplexing method which provides simultaneous detection of all recoil velocities, both speed and angle, for the detected product.[29] Furthermore, the images can be directly deconvoluted to yield the velocity–flux contour maps that summarize the dynamics. This deconvolution does not require the simplifying assumption of uncoupled translational energy and angular distributions usually employed in analyzing reactive scattering experiments, so the imaging experiments thus directly reveal the genuine double differential cross sections, $d^2\sigma/dE_T\, d\theta$. Another advantage of the imaging technique, particularly in the present studies, is the absence of any kinematic limitations on the reactions. Products scattering much faster or much slower than the beams themselves may be easily detected.

Very recently we performed the first experiment utilizing velocity map imaging[30] (VELMI) to study the reaction dynamics of the $O(^1D) + D_2 \rightarrow OD + D$ system.[31] Despite the advantages of the crossed beam imaging technique, there have been relatively few such studies.[32,33] Almost all have been performed using $1 + 1$ REMPI. While there are many more species that could be detected using $2 + 1$ REMPI, sensitivity issues (small interaction volume owing to the tight laser focus, low cross sections) have precluded their use except in a few recent cases of inelastic scattering. Recently, groups at Cornell[34–37] and Berkeley[20,21] have used VUV radiation to perform one-photon photoionization detection of polyatomic radical fragments from bimolecular reactions. The Berkeley group as mentioned earlier used tunable synchrotron radiation with a "traditional" crossed beam configuration to detect hydrocarbon radicals formed in bimolecular reactions of Cl with propane and n-pentane. The Cornell group has pioneered the use of 157 nm radiation generated by the F_2 excimer laser to photoionize products formed in metal–hydrocarbon bimolecular reactions. We adapted the latter technique to our crossed beam velocity map imaging experiment. Here we present results for the reaction of Cl with methanol, ethanol, and 2-propanol.

Experimental

The crossed molecular beams apparatus (Fig. 1) has been described in detail in recent publications from our group.[31,38] The Cl beam was generated by photodissociation of oxalyl chloride [$(ClCO)_2$] seeded in He, using the 193 nm output of an ArF excimer laser (60 mJ, 10 Hz, Lambda Physik) at the nozzle of a Proch–Trickl piezoelectric pulsed valve.[39] The molecular beam of $(ClCO)_2$ was generated by passing helium through a bubbler containing oxalyl chloride, held at 6 °C. The photodissociation dynamics of oxalyl chloride have recently been examined in our laboratory, and photodissociation at 193 nm yields predominantly Cl, Cl* and CO.[40] The Cl atom beam velocity and spread were monitored using $(2 + 1)$ REMPI of $Cl(^2P_{3/2})$ *via* the $4p^2D_{3/2} \leftarrow\leftarrow 3p^2P_{3/2}$ transition at 235.336 nm.[41] The UV photodissociation of oxalyl chloride also generates the spin–orbit excited $Cl^*(^2P_{1/2})$ which was monitored using the $4p^2P_{1/2} \leftarrow\leftarrow 3p^2P_{1/2}$ transition at 235.205 nm. The Cl*/Cl ratio was 1 : 50 and 1 : 62 for oxalyl chloride seeding in He and Ar respectively, or better than 98% ground state Cl, using relative linestrengths for the transitions as discussed in ref. 38. We believe that the efficient quenching is likely induced by many Cl–CO collisions. The speed ratio ($v/\Delta v$, FWHM) for the Cl beam was 5.8 (in He) and 2.3 (in Ar). The alcohol (methanol, ethanol, 2-propanol) seeded 2% in He was expanded through another Proch–Trickl pulsed valve, collimated by a single skimmer, and the beams were allowed to interact on the axis of the velocity focusing time-of-flight mass spectrometer. For the ethanol experiments the collision energy was reduced by seeding the oxalyl chloride in Ar. The speed ratio for the alcohol beams was greater than 12 in all cases.

Light from a 157 nm excimer laser (1–2 mJ, 10 Hz, Lambda Physik) was focused loosely into the interaction region of the two crossed beams and used to ionize the hydroxyalkyl radical reaction product. The ions were accelerated toward a 80 mm diameter dual microchannel plate (MCP) detector coupled to a fast phosphor screen (P-47) and imaged on a fast scan charge-coupled device camera with integrating video recorder (Data Design AC-101M). The ion yields were far below levels at which space charge effects would play a role. Camera threshold and gain were adjusted in conjunction with a binary video look-up table to perform integration of single ion hits on the MCP free of video noise. The recorded image is actually a two-dimensional (2-D) projection of the nascent three-dimensional (3-D) velocity distribution, and established tomographic techniques[29] were used to reconstruct the 3-D distribution. Typical accumulation time for a single collision energy was about 30 minutes.

Fig. 2 shows a raw image of the product formed at mass 45, CH_3CHOH, from the reaction of Cl with ethanol probed with 157 nm laser light. The relative velocity vector is vertical in the plane of the figure, and the Newton diagram for the scattering process has been superimposed on the image. There is substantial photodissociation of ethanol at 157 nm which also produces CH_3CHOH. This shows up as the small ring centered at the ethanol beam. As is immediately apparent from the image, this creates a problem in extracting information for the most sharply forward-scattered products relative to the incoming alcohol beam. We subtract an image recorded with the 193 nm laser off, from one with the laser on, to isolate the reactive scattering image and remove the photodissociation contribution. Unfortunately, the intense photochemical signal creates substantial noise and corresponding uncertainty in the reactive flux formed between 0 and 50°. For the present data,

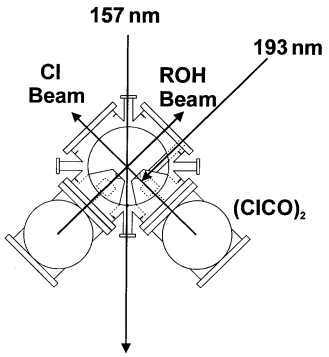

Fig. 1 Schematic of crossed beam VELMI apparatus.

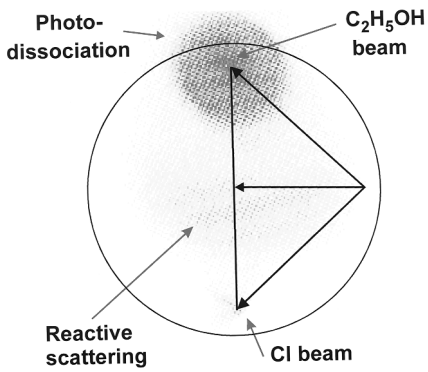

Fig. 2 Raw image for 1-hydroxyethyl (CH_3CHOH) radical product of crossed beam Cl–C_2H_5OH reaction at 9.7 kcal mol^{-1} collision energy.

we feel the subtractions do not yield reliable results in the region of the photodissociation signal, and we omit the unreliable region of the distributions. Fortunately, this is limited to the most sharply forward portion of the distributions, where the fraction of the product flux appears to be small anyway. The cylindrical symmetry of the experiment justifies the use of the inverse Abel transform method to reconstruct the full 3-D distributions, so that this analysis is, in effect, a direct inversion of the experimental data. However, this approach does not deconvolute the beam velocity spreads or the angular divergence of the molecular beams. The images are also subject to some additional distortion from the fact that the scattering may occur well before the probe laser arrives, so that products with a slow laboratory velocities are detected more efficiently than fast products. We take several steps to minimize this problem. We employ intense, sharp pulses using piezo valves and a photolytic Cl atom source, so that the arrival of the Cl beam pulse is very abrupt. Furthermore, we probe immediately after the arrival of the Cl beam pulse, even though the signal there is not a maximum. Finally, our one photon probe laser interaction volume is large relative to the beam interaction volume. Monte Carlo simulations of the detection efficiency as a function of the recoil velocity[31] show that we will not be subject to significant distortion under our experimental conditions; this is confirmed by the appearance of the raw scattering image in Fig. 2.

Results

Cl + methanol

The reaction of Cl with methanol can proceed *via* two channels:

$$Cl + CH_3OH \rightarrow CH_3O + HCl \quad \Delta H = +2.4 \text{ kcal mol}^{-1} \quad (1)$$

$$\rightarrow CH_2OH + HCl \quad \Delta H = -6.8 \text{ kcal mol}^{-1} \quad (2)$$

channels (1) and (2) forming the methoxy and hydroxymethyl radicals respectively. The branching ratio for the latter channel has been found experimentally[42] to be close to unity, 0.95. The ionization potential (IP) for CH_3O is 10.42 eV[43] (and the CH_3O^+ ion is unstable[44]) so that we will not be sensitive to this channel. However the IP for CH_2OH is 7.56 eV,[45] so that single photon ionization using the 157 nm laser light (7.9 eV) will readily probe this product from channel (2) above. Fig. 3 shows an image of the product formed at mass 31, CH_2OH^+, from the reaction of Cl with methanol. The relative velocity vector is vertical in the plane of the figure, and the Newton diagram for the scattering process has been superimposed on the image.

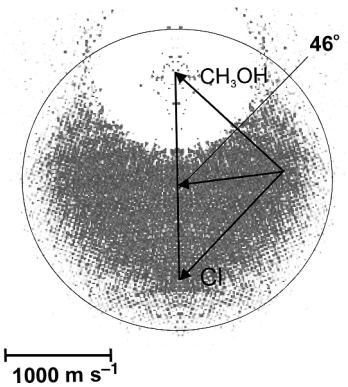

Fig. 3 Data image for hydroxymethyl (CH_2OH) radical product of crossed beam Cl–CH_3OH reaction at 8.7 kcal mol^{-1} collision energy.

At a collision energy E_{coll} of 8.7 kcal mol^{-1}, there is 15.5 kcal mol^{-1} energy available to be distributed into translation and the internal energy of the products. The outer ring in Fig. 3 shows the maximum recoil speed allowed for the CH_2OH radical; there is reactive flux virtually to the limit of available energy in the sideways and backward direction. The center-of-mass (CM) angular distributions [dΦ/d(2)] extracted from the images are shown in the lower panel of Fig. 4. There is substantial sideways scattering—the ratio of sideways (45–135°) to backward (135–180°) is 1.75. The upper panel in Fig. 4 shows the translational energy distribution obtained from the reconstructed data at $E_{coll} = 8.7$ kcal mol^{-1}. The maximum available energy is indicated in the figure. The average translational energy released is 6.1 kcal mol^{-1}, or 39% of the available energy.

Cl + ethanol

The abstraction of an H atom from ethanol by the Cl atom can give rise to three different radicals as shown below:

$$C_2H_5OH + Cl$$

$$\rightarrow CH_3CHOH + HCl \quad \Delta H = -9.3 \text{ kcal mol}^{-1} \quad (3)$$

$$\rightarrow CH_2CH_2OH + HCl \quad \Delta H = +0.5 \text{ kcal mol}^{-1} \quad (4)$$

$$\rightarrow CH_3CH_2O + HCl \quad \Delta H = +4.5 \text{ kcal mol}^{-1} \quad (5)$$

In our experiment we will not observe the ethoxyl radical channel (5), since its ionization energy of 10.29 eV[46] is way above that available from a 157 nm photon (7.89 eV). The ionization energies (IE) for the 1-hydroxyethyl and 2-hydroxyethyl radicals formed in processes (3) and (4) are 6.64 eV[47] and ~8.2 eV[46] respectively. However the IE for 2-hydroxyethyl is by no means conclusive. Ruscic and Berkowitz[46] quote a figure of 8.18 ± 0.08 eV, but they infer an IP of ~7.7 eV depending on the thermodynamic cycle and bond dissociation energies employed in generating the result. A G-2 theoretical result[48] posits 7.58 eV as the adiabatic ionization energy for the 2-hydroxyethyl radical. Khatoon *et al.*[49] carried out an end product analysis experiment to measure the rates of this reaction and also derive the branching ratio for the formation of the three different radicals. They conclude that, for the reaction of Cl with alcohols, no abstraction from the OH group was observed and that the abstraction from the alkyl groups followed the thermodynamically favored route

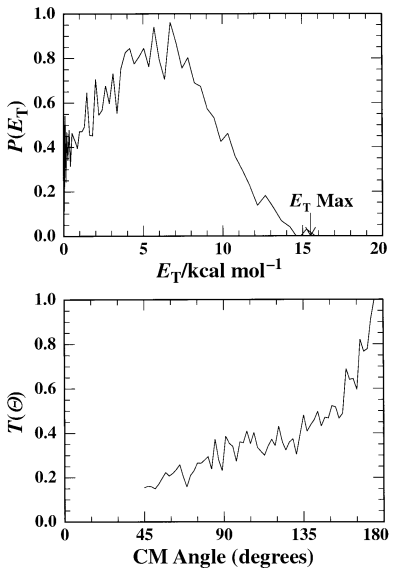

Fig. 4 Translational energy (top) and angular distribution (bottom) for hydroxymethyl radical from image data in Fig. 3. Forward scattering (0°) corresponds to the methanol beam direction.

by forming mainly secondary radicals. With this in mind we can tentatively say that the mass 45 detected is the 1-hydroxyethyl radical.

Reactive scattering experiments with ethanol were performed at two collision energies $E_{coll} = 6.0$ and 9.7 kcal mol^{-1}. Fig. 5A shows the raw image for 6.0 kcal mol^{-1} and as indicated previously for the methanol results the Newton diagram is superimposed on the image. The reactive flux is predominantly in the backward hemisphere. When the collision energy is increased to 9.7 kcal mol^{-1}, there is enhanced sideways scattering, and the raw image shown in Fig. 5B begins to resemble the methanol system. However, for ethanol at both collision energies the reactive flux does not extend out to the thermodynamic limit. The average translational energy release is 38% and 32% of the available energy for $E_{coll} = 6.0$ and 9.7 kcal mol^{-1}, respectively. The upper panel in Fig. 6 shows the translational energy distribution obtained from the reconstructed data at $E_{coll} = 6.0$ and 9.7 kcal mol^{-1}. The corresponding angular distributions are shown in the lower panel, normalized to the same maximum in the backward direction. As was apparent in the raw images, we see a significant enhancement in sideways scattering with an increase in collision energy. There is also substantial coupling between translational energy release and corresponding angular distributions. Fig. 7 compares the translational energy release for the sideways (50–130°) and backward (130–180°) components at a collision energy of 6.0 kcal mol^{-1}. The average energy release for the sideways scattering is 4.7 kcal mol^{-1}; the backward scattering is faster, with an average of 6.6 kcal mol^{-1} translational energy.

Cl + isopropanol

An image recorded at mass 59, corresponding to $(CH_3)_2COH^+$, is shown in Fig. 8. The ionization energies for the possible product radicals are not available, except for 9.2 eV for the product of hydroxyl H abstraction, the 1-methyl ethoxy radical.[50] However, analogy to the systems above suggests a much lower IE for the $(CH_3)_2COH$ radical, and we believe this to be the most likely candidate for our detected product in this reaction. The scattering is predominantly in the backward hemisphere and the image resembles the ethanol case for low collision energy. Fig. 9 shows the translational energy release and angular distributions. Again we see that the energy release is not to the thermodynamic limit.

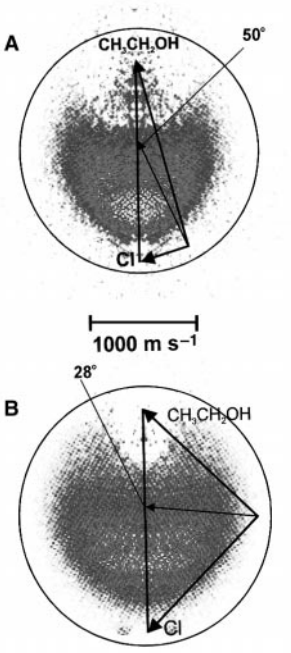

Fig. 5 Data images for 1-hydroxyethyl (CH_3CHOH) radical product of crossed beam Cl–C_2H_5OH reaction at (A) 6.0 kcal mol^{-1} and (B) 9.7 kcal mol^{-1} collision energy.

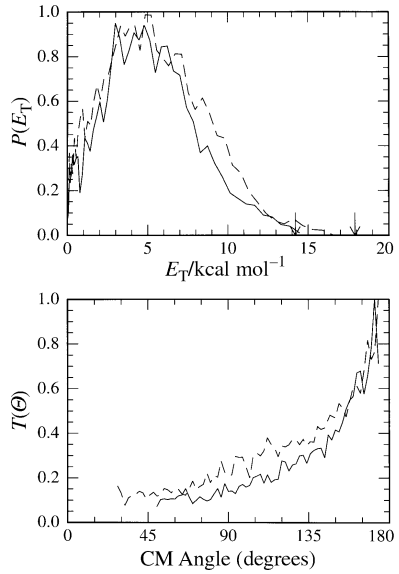

Fig. 6 Translational energy (top) and angular distribution (bottom) for 1-hydroxyethyl radical from image data in Fig. 5. Forward scattering (0°) corresponds to the ethanol beam direction. Solid line $E_{coll} = 6.0$ kcal mol^{-1}, dashed line $E_{coll} = 9.7$ kcal mol^{-1}.

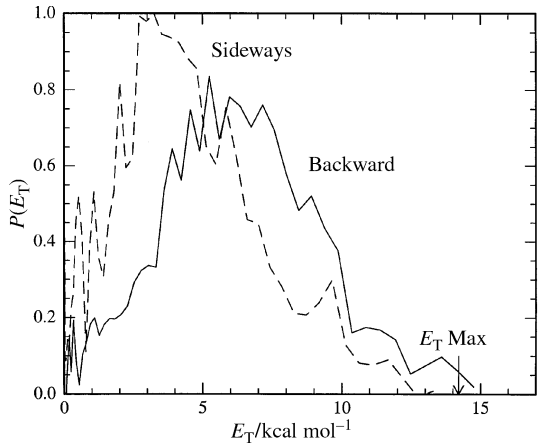

Fig. 7 Translational energy distribution for sideways (dashed line) and back-scattered (solid line) component of 1-hydroxyethyl radical product of crossed beam Cl–C_2H_5OH reaction at 6.0 kcal mol^{-1}.

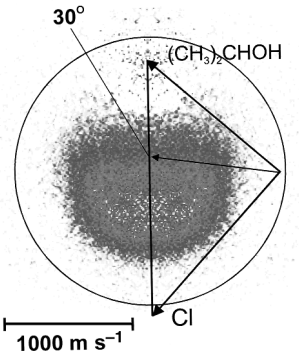

Fig. 8 Data image for hydroxyisopropyl [$(CH_3)_2COH$] radical product of crossed beam Cl–2-C_3H_7OH reaction at 11.9 kcal mol^{-1} collision energy. Forward scattering (0°) corresponds to the propanol beam direction.

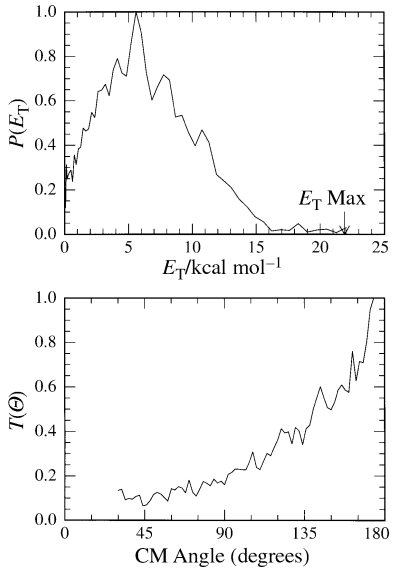

Fig. 9 Translational energy (top) and angular distribution (bottom) for hydroxyisopropyl radical from image data in Fig. 8. Forward scattering (0°) corresponds to the 2-propanol beam direction.

Table 1 summarizes the results for all the alcohols studied in this experiment. All the translational energy distributions peak around 6 kcal mol^{-1}, irrespective of the alcohol reagent and collision energy. Another common thread is that the fraction of energy going into translation is similar for all the alcohols.

Discussion

The reaction of methanol with chlorine atoms has been studied in a number of laboratories using traditional kinetic methods[51] and the consensus is that the hydroxymethyl radical formation channel is predominant. The rate of reaction is moderately fast, (5.3–6.3) $\times$ 10^{-11} cm^3 molecule^{-1} s^{-1}, with no appreciable barrier. There has been no experimental study on the dynamics of H abstraction from methanol. However Jodkowski *et al.*[51] have performed *ab initio* calculations at different levels of theory and using several basis sets to characterize stationary points on the potential surface for the reaction of Cl with CH_3OH. They found several minima, including one in the entrance channel corresponding to Cl attaching to the O atom, and another in the exit channel resembling a hydrogen bonded complex between HCl and CH_2OH, with the latter representing the minimum point on the surface, 10.0 kcal mol^{-1} below the reactants. The presence of these minima led them to suggest that reaction occurs *via* formation of an intermediate complex similar to the CH_3OH + F reaction.[52] No exit barrier was found in their calculation for the CH_2OH + HCl channel. However, they generated only a few stationary points on the surface and did not explicitly consider the reaction path. Our results clearly show the importance of a direct reaction mechanism, at least at our 8.7 kcal mol^{-1} collision energy, since we see exclusively sideways–backward scattered distributions. Although in the present studies we are not sensitive to the sharply forward–scattered products, in all cases we can rule out the forward-backward symmetry characteristic of collision complexes. We interpret all of the observed angular distributions as implying direct, close (small but non-vanishing impact parameter) collisions.

Khatoon *et al.*[49] studied the kinetics and mechanism of reaction of Cl with ethanol (1.2 $\times$ 10^{-10} cm^3 molecule^{-1} s^{-1}) and 1- and 2-propanol. For the reaction of Cl atoms with alcohols, the authors saw no abstraction from the OH group; abstraction from the alkyl groups followed the thermodynamically favored route by forming mainly secondary radicals. Edelbuttel-Einhaus *et al.*[53] report a rate constant of 7.84 $\times$ 10^{-11} cm^3 molecule^{-1} s^{-1} and obtain a branching ratio of 1 : 20 between reactions (4) and (3), confirming that the 1-hydroxyethyl radical is predominantly formed.

The scattering studies on ethanol allow us to compare the effect of collision energy. At low collision energy, scattering is predominantly in the backward hemisphere. With an increase in collision energy the scattering is enhanced in the sideways direction with no concomitant increase in the translational energy release. The angular distribution for ethanol at the higher collision energy begins to resemble that of methanol, suggesting that larger impact parameter collisions begin to play a role, or deviations from collinearity may be more important. The translational energy release is reduced in the sideways direction, implying greater internal energy in the larger impact parameter collisions. This is consistent with greater rotational excitation for these sideways scattered products.

The energies of the C–H bonds in ethanol and propane are very similar; furthermore, the structures resemble each other. This allows us to compare the results for Cl–C_2H_5OH with Cl–C_3H_8. We do not observe the large impact parameter dominated fast forward–sideways scattering reported in the case of propane. However, for the low impact parameter sideways–backward scattering there is qualitative agreement with our results. Blank *et al.*[20] saw strong coupling between their angular and translational energy distributions—again this is in agreement with our observations. These authors found a much larger fraction of available energy in translation than in the Cl–ethanol reaction, and this fraction changed little with collision energy ($\langle E_T \rangle / E_{avl} = 0.53$, 0.52, 0.48 for $E_{coll} = 8.0$, 11.5, 31.6 kcal mol^{-1}). An examination of column 5 in Table 1 shows qualitatively similar behavior.

Following in a similar vein, scattering for the Cl–C_3H_7OH system should resemble the Cl–C_5H_{12} system. As mentioned in the Introduction, Hemmi and Suits[21] invoked the participation of the carbon skeleton in the scattering process to account for the substantial internal energy deposited in the hydrocarbon radical fragment. In the case of the Cl–isopropanol system our angular distributions are qualitatively quite similar to the backward scattering [channel (2)] reported in the Cl–C_5H_{12} system. They saw a broad backward scattering distribution with about 35% of the available energy being deposited into product translation; in the Cl–C_3H_7OH system we observe 31%. And just as in the propane case,

Table 1 Summary of results

ROH	E_{coll}[a] kcal mol^{-1}	E_{avl}[b] kcal mol^{-1}	$\langle E_T \rangle$[c] kcal mol^{-1}	f_T[d]	$r_{side/back}$[e]
CH_3OH	8.7	15.5	6.1	0.39	1.75
C_2H_5OH	6.0	14.2	5.4	0.38	1.23
C_2H_5OH	9.7	17.9	5.7	0.32	1.64
C_3H_7OH	11.9	21.9	6.8	0.31	1.33

[a] Collision energy. [b] Total energy available. [c] Average translational energy release. [d] Fraction of total energy appearing in translation. [e] Ratio of side ways scattered to back-scattered flux (see text).

Hemmi and Suits observed a distinct forward–sideways scattered component with almost all the available energy being deposited into product translation.

It is surprising, given the similarity in the sideways–backward scattering between the Cl–alcohol and Cl–hydrocarbon systems, that we do not observe the analogous fast forward–sideways scattering component seen by Suits and co-workers in their Cl–hydrocarbon experiments. As mentioned before we cannot extract quantitative information about sharply forward-scattered products since the extensive photodissociation of the parent alcohol obscures the distribution in the range 0–45°. However any strong forward scattering, even in the unlikely event that it is confined to this region, will be superimposed on the photodissociation signal and this should be apparent in our experiment. A possible reconciliation of the difference between our experiment and those performed on the Cl–hydrocarbon systems may lie in the source of Cl atoms used in the two sets of experiments. We used a photolytic source and have carefully characterized the Cl beam to be of predominantly ground state character. In the Cl–hydrocarbon experiments[20,21] the Cl atom beam was generated by thermal dissociation of Cl_2 in a heated nozzle maintained at 1500–1550 °C. A Boltzmann distribution as stated by the authors predicts that *ca.* 15% of the chlorine atoms will be formed in spin–orbit excited state, $Cl(^2P_{1/2})$. While the excited state component of the Cl beam was not explicitly determined, the authors assumed that the supersonic expansion would relax the spin–orbit excited component of the beam. Recently Liu and co-workers have seen enhanced reactivity with spin–orbit excited Cl (ref. 54) and F (ref. 55) atoms. They find that the spin–orbit excited atoms show very different dynamical behavior compared to their ground state counterparts. We tentatively suggest that the forward scattering seen in the crossed beam Cl–hydrocarbon systems may arise from the participation of the spin–orbit excited component of their Cl. Efforts are under way in this laboratory to study the effect of spin–orbit excitation on the reaction dynamics with alcohols and hydrocarbons.

There is also the possibility, since we use single photon ionization, that internal excitation of the product detected might bias our sensitivity. It is known that internal excitation of species usually lowers the ionization potential—in our case this would lead to detecting highly vibrationally excited products more efficiently. However an experimental complication in our studies—the alcohol photochemistry—suggests that we are not subject to such bias. We measured the translational energy release of CH_2OH and CH_3CHOH formed in the 157 nm photodissociation of CH_3OH and CH_3CH_2OH respectively. In both cases we found the energy release was to the thermodynamic limit. If we were biased in our detection sensitivity we would not be as sensitive to internally cold products. We are thus reassured that we are not subject to serious internal energy bias in our VUV photoionization crossed beam velocity map imaging experiment. We intend future measurements to verify this assumption.

These results demonstrate the power of VELMI combined with single photon VUV ionization. Work is currently under way in our laboratory on reactions with other alcohols, and analogous reactions of O and OH should be quite feasible. With judicious choice of chemical system and probe light sources, the detailed and systematic investigations of the dynamics of many polyatomic reactions should be routine.

Acknowledgements

This paper is fondly dedicated to the memory of the late Professor Roger W. Grice, a continuing inspiration to the practitioners of the crossed molecular beams technique. We thank Mr. K. Rodriguez (U*STAR undergraduate student training in academic research) and Mr. J. McFarland for technical assistance, and Professor C. B. Moore for loan of the video integration system. This work was supported by the Director, Office of Energy Research, Office of Basic Energy Sciences, Chemical Sciences Division of the US Department of Energy under contract No. DE-ACO3-76SF00098.

References

1 P. Andresen and A. C. Luntz, *J. Chem. Phys.*, 1980, **72**, 5842.
2 A. C. Luntz and P. Andresen, *J. Chem. Phys.*, 1980, **72**, 5851.
3 K. Kleinermanns and A. C. Luntz, *J. Chem. Phys.*, 1982, **77**, 3533.
4 K. Kleinermanns and A. C. Luntz, *J. Chem. Phys.*, 1982, **77**, 3537.
5 K. Kleinermanns and A. C. Luntz, *J. Chem. Phys.*, 1982, **77**, 3774.
6 N. J. Dutton, J. W. Farthing, I. W. Fletcher and J. C. Whitehead, *Mol. Phys.*, 1983, **50**, 347.
7 N. J. Dutton, I. W. Fletcher and J. C. Whitehead, *Mol. Phys.*, 1984, **52**, 475.
8 G. M. Sweeney, A. Watson and K. G. McKendrick, *J. Chem. Phys.*, 1997, **106**, 9172.
9 G. M. Sweeney and K. G. McKendrick, *J. Chem. Phys.*, 1997, **106**, 9182.
10 W. R. Simpson, A. J. Orr-Ewing and R. N. Zare, *Chem. Phys. Lett.*, 1993, **212**, 163.
11 W. R. Simpson, T. P. Rakitzis, S. A. Kandel, A. J. Orr-Ewing and R. N. Zare, *J. Chem. Phys.*, 1995, **103**, 7313.
12 W. R. Simpson, T. P. Rakitzis, S. A. Kandel, T. Lev-On and R. N. Zare, *J. Phys. Chem.*, 1996, **100**, 7938.
13 J. H. Park, Y. S. Lee, J. F. Hershberger, J. M. Hossenlopp and G. W. Flynn, *J. Am. Chem. Soc.*, 1992, **114**, 58.
14 T. P. Rakitzis, S. A. Kandel, T. Lev-On and R. N. Zare, *J. Chem. Phys.*, 1997, **107**, 9392.
15 S. A. Kandel, T. P. Rakitzis, T. Lev-On and R. N. Zare, *J. Phys. Chem. A*, 1998, **102**, 2270.
16 S. A. Kandel, T. P. Rakitzis, T. Lev-On and R. N. Zare, *J. Chem. Phys.*, 1996, **105**, 7550.
17 D. F. Varley and P. J. Dagdigian, *J. Phys. Chem.*, 1995, **99**, 9843.
18 D. F. Varley and P. J. Dagdigian, *Chem. Phys. Lett.*, 1996, **255**, 393.
19 D. F. Varley and P. J. Dagdigian, *J. Phys. Chem.*, 1996, **100**, 4365.
20 D. A. Blank, N. Hemmi, A. G. Suits and Y. T. Lee, *Chem. Phys.*, 1998, **231**, 261.
21 N. Hemmi and A. G. Suits, *J. Chem. Phys.*, 1998, **109**, 5338.
22 D. Grosjean, *J. Braz. Chem. Soc.*, 1997, **8**, 433.
23 S. O. Lowry and R. S. Devoto, *Combust. Sci. Technol.*, 1976, **12**, 177.
24 T. B. Reed and R. M. Lerner, *Science*, 1973, **182**, 1299.
25 N. Goldstein and J. R. Wiesenfeld, *J. Chem. Phys.*, 1983, **78**, 6725.
26 H. Umemoto, K. Kongo, S. Inaba, Y. Sonoda, T. Takayanagi and Y. Kurosaki, *J. Phys. Chem. A*, 1999, **103**, 7026.
27 S. E. Bradforth, D. W. Arnold, R. B. Metz, A. Weaver and D. M. Neumark, *J. Phys. Chem.*, 1991, **95**, 8066.
28 M. Ahmed, D. S. Peterka and A. G. Suits, *Chem. Phys. Lett.*, 1999 in the press.
29 B. J. Whitaker, in *Research in Chemical Kinetics*, ed. R. C. Compton and G. Hancock, Elsevier, Amsterdam, 1993, vol. I.
30 A. T. J. B. Eppink and D. H. Parker, *Rev. Sci. Instrum.*, 1997, **68**, 3477.
31 M. Ahmed, D. S. Peterka and A. G. Suits, *Chem. Phys. Lett.*, 1999, **301**, 372.
32 A. G. Suits, L. S. Bontuyan, P. L. Houston and B. J. Whitaker, *J. Chem. Phys.*, 1992, **96**, 8618.
33 T. N. Kitsopoulos, M. A. Buntine, D. P. Baldwin, R. N. Zare and D. W. Chandler, *Science*, 1993, **260**, 1605.
34 P. A. Willis, H. U. Stauffer, R. Z. Hinrichs and H. F. Davis, *J. Chem. Phys.*, 1998, **108**, 2665.
35 P. A. Willis, H. U. Stauffer, R. Z. Hinrichs and H. F. Davis, *J. Phys. Chem. A*, 1999, **103**, 3706.
36 P. A. Willis, H. U. Stauffer, R. Z. Hinrichs and H. F. Davis, *Rev. Sci. Instrum.*, 1999, **70**, 2606.
37 H. U. Stauffer, R. Z. Hinrichs, P. A. Willis and H. F. Davis, *J. Chem. Phys.*, 1999, **111**, 4101.
38 M. Ahmed, D. Blunt, D. Chen and A. G. Suits, *J. Chem. Phys.*, 1997, **106**, 7617.
39 D. Proch and T. Trickl, *Rev. Sci. Instrum.*, 1989, **60**, 713.
40 N. Hemmi and A. G. Suits, *J. Phys. Chem. A*, 1997, **101**, 6633.
41 S. Arepalli, N. Presser, D. Robie and R. J. Gordon, *Chem. Phys. Lett.*, 1985, **118**, 88.
42 S. Dobe, T. Berces, F. Temps, H. G. Wagner and H. Ziemer, in *Proceedings of the 25th Symposium (International) on Combustion*, Combustion Institute, Pittsburgh, 1994, p. 775.

43 B. Ruscic and J. Berkowitz, *J. Phys. Chem.*, 1993, **97**, 11451.
44 B. Ruscic and J. Berkowitz, *J. Chem. Phys.*, 1991, **95**, 4033.
45 S. G. Lias, J. E. Bartmess, J. F. Liebman, J. L. Holmes, R. D. Levin and W. G. Mallard, in *NIST Chemistry WebBook*, *NIST Standard Reference Database Number 69* (http://webbook.nist.gov), ed. W. G. Mallard and P. J. Linstrom, National Institute of Standards and Technology, Gaithersburg, MD, 1998.
46 B. Ruscic and J. Berkowitz, *J. Chem. Phys.*, 1994, **101**, 10936.
47 J. M. Dyke, A. P. Groves, E. P. F. Lee and M. H. Z. Niavaran, *J. Phys. Chem. A*, 1997, **101**, 373.
48 L. A. Curtiss, D. J. Lucas and J. A. Pople, *J. Chem. Phys.*, 1995, **102**, 3292.
49 T. Khatoon, J. Edelbuttel-Einhaus, K. Hoyermann and H. G. Wagner, *Ber. Bunsen-Ges. Phys. Chem.*, 1989, **93**, 626.
50 J. M. Williams and W. H. Hamill, *J. Chem. Phys.*, 1968, **49**, 4467.
51 J. T. Jodkowski, M. T. Rayez, J. C. Rayez, T. Berces and S. Dobe, *J. Phys. Chem. A*, 1998, **102**, 9230.
52 J. T. Jodkowski, M. T. Rayez, J. C. Rayez, T. Berces and S. Dobe, *J. Phys. Chem. A*, 1998, **102**, 9219.
53 J. Edelbuttel-Einhaus, K. Hoyermann, G. Rohde and J. Seeba, *Proc. 24th Symp.* (*Int.*) *Combust.*, Combustion Institute, Pittsburgh, PA, 1992, p. 661.
54 S. H. Lee, L. H. Lai, K. P. Liu and H. Chang, *J. Chem. Phys.*, 1999, **110**, 8229.
55 K. P. Liu, personal communication.

Paper a907877k